

# Role of the Conserved SRLFDQFFG Region of $\alpha$ -Crystallin, a Small Heat Shock Protein

EFFECT ON OLIGOMERIC SIZE, SUBUNIT EXCHANGE, AND CHAPERONE-LIKE ACTIVITY\*

Received for publication, July 14, 2003, and in revised form, September 9, 2003  
Published, JBC Papers in Press, October 7, 2003, DOI 10.1074/jbc.M307523200

Saloni Yatin Pasta‡, Bakthisaran Raman, Tangirala Ramakrishna, and Ch. Mohan Rao§

From the Centre for Cellular and Molecular Biology, Hyderabad 500 007, India

Small heat shock proteins (sHsps) are necessary for several cellular functions and in stress tolerance. Most sHsps are oligomers; intersubunit interactions leading to changes in oligomeric structure and exposure of specific regions may modulate their functioning. Many sHsps, including  $\alpha$ A- and  $\alpha$ B-crystallin, contain a well conserved SRLFDQFFG sequence motif in the N-terminal region. Sequence-based prediction shows that it exhibits helical propensity with amphipathic character, suggesting that it plays a critical role in the structure and function of  $\alpha$ -crystallins. In order to investigate the role of this motif in the structure and function of sHsps, we have made constructs deleting this sequence from  $\alpha$ A- and  $\alpha$ B-crystallin, overexpressed, purified, and studied these engineered proteins. Circular dichroism spectroscopic studies show changes in tertiary and secondary structure on deletion of the sequence. Glycerol density gradient centrifugation and dynamic light scattering studies show that the multimeric size of the mutant proteins is significantly reduced, indicating a role for this motif in higher order organization of the subunits. Both deletion mutants exhibit similar oligomeric size and increased chaperone-like activity. Urea-induced denaturation study shows that the SRLFDQFFG sequence contributes significantly to the structural stability. Fluorescence resonance energy transfer studies show that the rate of exchange of the subunits in the  $\alpha$ Adel-crystallin oligomer is higher compared with that in the  $\alpha$ A-crystallin oligomer, suggesting that this region contributes to the oligomer dynamics in addition to the higher order assembly and structural stability. Thus, our study shows that the SRLFDQFFG sequence is one of the critical motifs in structure-function regulation of  $\alpha$ A- and  $\alpha$ B-crystallin.

$\alpha$ -Crystallin, a multimeric protein composed of two types of subunits,  $\alpha$ A- and  $\alpha$ B-crystallin, is abundantly present in the eye lens (1). Both  $\alpha$ A- and  $\alpha$ B-crystallin have subunit molecular masses of ~20 kDa each, share high sequence homology (2), can form homomultimers (3, 4), and are known to be present in other nonlenticular tissues as well (5, 6). Ingolia and Craig (7), while comparing the sequences of four small heat shock proteins from *Drosophila*, discovered the remarkable similarity between  $\alpha$ B-crystallin and small heat shock proteins.

Prompted by this sequence similarity, Klemenz *et al.* (8) investigated the expression of  $\alpha$ -crystallin under heat shock and concluded that indeed  $\alpha$ -crystallin is a heat shock protein. Horwitz (9) subsequently showed that  $\alpha$ -crystallin prevents aggregation of other proteins like other heat shock proteins.

$\alpha$ B-crystallin and not  $\alpha$ A-crystallin is stress-inducible. Its levels increase under stress such as heat shock, ischemia, oxidation, and infection and in various disease conditions (10–12).  $\alpha$ A- and  $\alpha$ B-crystallin, either in their hetero- or homo-oligomeric states, exhibit molecular chaperone-like properties in preventing protein aggregation (4, 9, 13, 14).  $\alpha$ -Crystallin binds to partially unfolded, aggregation-prone intermediate states of proteins having molten globule-like properties via appropriately placed hydrophobic binding sites (15–18). Studies from our laboratory (13, 19, 20) and subsequently from other laboratories (21, 22) have shown that the chaperone-like activity of  $\alpha$ -crystallins is temperature-dependent. The observed temperature-induced enhancement of activity involves a structural transition that enhances the activity by increasing or favorably reorganizing the hydrophobic substrate-binding surfaces (13, 14, 19–22). Its differential and reversible interaction with early unfolding, refolding-competent intermediates of target proteins decreases their partitioning into aggregation-prone late unfolding intermediates (18, 23). This appears to be important in the observed protection offered by  $\alpha$ -crystallin to enzymes from heat-induced inactivation (23–26).  $\alpha$ -Crystallins/sHsps<sup>1</sup> are believed to serve as reservoirs to maintain partially unfolded target proteins in a folding-competent state, capable of subsequent refolding unassisted or by other chaperone systems (27).

Markedly decreased chaperone-like activity and altered structure (28, 29) due to the mutations of the conserved arginine residue, R120G in  $\alpha$ B-crystallin and R116C in  $\alpha$ A-crystallin, manifest in desmin-related myopathy and congenital cataract, respectively (30, 31). The R116C mutant of  $\alpha$ A-crystallin offers reduced protection to apoptosis in lens epithelial cells subjected to UV stress (32). These and other similar observations suggest that the chaperone-like activity of  $\alpha$ -crystallin is important in normal cellular function as well as in stress tolerance. Although growing evidence implicates the functional importance of  $\alpha$ -crystallins in many cellular processes (27), knowledge about its structure-function relationship remains elusive largely due to the lack of an x-ray crystal structure or NMR solution structure.

Sequence comparison between several sHsps shows an evolutionarily conserved sequence of about 80–100 amino acids,

\* The costs of publication of this article were defrayed in part by the payment of page charges. This article must therefore be hereby marked "advertisement" in accordance with 18 U.S.C. Section 1734 solely to indicate this fact.

‡ Supported by a Senior Research Fellowship from the Council of Scientific and Industrial Research, New Delhi, India.

§ To whom correspondence should be addressed. Tel.: 91-40-2719-2543; Fax: 91-40-2716-0591; E-mail: mohan@ccmb.res.in.

<sup>1</sup> The abbreviations used are: sHsps, small heat shock protein; FRET, fluorescence resonance energy transfer; DTT, dithiothreitol; AIAS, 4-acetamido-4'-((iodoacetyl)amino)stilbene-2,2'-disulfonic acid; LYI, lucifer yellow iodoacetamide; MOPS, 4-morpholinepropanesulfonic acid; bis-ANS, 1,1'-bi(4-anilino)naphthalenesulfonic acid.

called the “ $\alpha$ -crystallin domain” (33), flanked by the N-terminal domain and the C-terminal region (generally termed as C-terminal extension). The C-terminal region is largely unstructured and is believed to have a solubilizing role, since it contains many charged residues (34). Our recent study showed that besides its solubilizing role, it could also influence the structure and the chaperone-like activity significantly (35). The differences in the N-terminal domains and the C-terminal extensions of sHsps may result in their differing oligomeric assembly, size, dynamics, and functions.

Deletion of the first 63 residues of the N-terminal domain of  $\alpha$ A-crystallin leads to a drastic reduction in the size of the protein to dimers or tetramers (36). However, truncation of the first 19 residues of the N-terminal domain of  $\alpha$ A-crystallin does not alter the size significantly; the rate of subunit exchange also does not change significantly (37). Besides the  $\alpha$ -crystallin domain, there are two notable regions (or motifs) that are conserved, especially among the mammalian sHsps: one in the N-terminal domain, RLFDQXFG, and another in the C-terminal extension, the IX(I/V) motif (33). However, the structural and functional significance of these regions is not understood. We therefore set out to investigate the role of the SRLFDQFFG sequence in the structure and chaperone-like activity of  $\alpha$ A- and  $\alpha$ B-crystallins by creating mutants that lack this sequence ( $\alpha$ Adel<sub>20–28</sub> and  $\alpha$ Bdel<sub>21–29</sub>; for simplicity termed  $\alpha$ Adel- and  $\alpha$ Bdel-crystallin henceforth). Our results demonstrate that deletion of this sequence results in significant decrease in the oligomeric size and stability toward urea-induced denaturation, indicating that this sequence is one of the determinants of the quaternary structure of  $\alpha$ -crystallins and contributes to the structural stability. Both the deletion mutants exhibit severalfold increased chaperone-like activity compared with that of  $\alpha$ A- and  $\alpha$ B-crystallin. Our results show that this region also contributes to the dynamics of subunit assembly as the  $\alpha$ Adel-crystallin exhibits a significantly increased rate of subunit exchange compared with the wild type protein as monitored by fluorescence resonance energy transfer (FRET).

#### EXPERIMENTAL PROCEDURES

**Materials**—pET-21a(+), T7 promoter and terminator primers were obtained from Novagen (Madison, WI), pBS(II)SK was from Stratagene, and insulin and bis-ANS were from Sigma. Sephacryl HR-300 was purchased from AP-Biotech. Dithiothreitol (DTT) was obtained from Sisco Research Laboratories (Mumbai, India). Fluorescence probes used in FRET experiments, namely the disodium salt of 4-acetamido-4'-(iodoacetyl)amino)stilbene-2,2'-disulfonic acid (AIAS) and dipotassium salt of lucifer yellow iodoacetamide (LYI), were purchased from Molecular Probes, Inc. (Eugene, OR).

**Creating Mutant  $\alpha$ Adel- and  $\alpha$ Bdel-crystallin**—Recombinant human  $\alpha$ A- and  $\alpha$ B-crystallin genes were cloned in pET-21a(+) as described earlier (28). These constructs were used as templates to generate the deletion mutants using PCR. For  $\alpha$ Adel-crystallin, two independent PCRs were performed using T7 promoter primer and the mutagenic primer 5'-GGGGTAGAAGGGCCCC-3' as one primer pair and 5'-GAGGGCCTTTTGGAGTATG-3' and T7 terminator primer as the second primer pair. Fragments of 137 and 588 bp generated in the PCR were digested using NdeI and HindIII, respectively, and cloned in the NdeI and HindIII sites of pET-21a(+) expression vector via a three-point ligation. The same strategy was employed for  $\alpha$ Bdel-crystallin using T7 promoter primer and 5'-GGGGGAGTGGAAAGGAAA-3' and 5'-GAGCACCTGTTGGAGTCT-3' and the T7 terminator primer to generate 140- and 532-bp fragments, respectively. These fragments were also three-point ligated into the NdeI and HindIII sites of pET-21a(+) expression vector. These constructs were verified by sequencing using a 3700 ABI automated DNA sequencer.

**Expression and Purification of the Recombinant Wild Type and Mutant Proteins**—The wild type and the mutant recombinant proteins were overexpressed in *Escherichia coli* BL21(DE3) cells. All the purification processes were performed using 50 mM Tris-HCl buffer (pH 7.4) containing 100 mM NaCl, 1 mM EDTA with 0.02% sodium azide (TNE). Bacterial cells were lysed in TNE buffer using lysozyme and then sonicated to shear the genomic DNA. The purification procedure for the

wild type and mutant  $\alpha$ A- and  $\alpha$ B-crystallin was essentially as described by Sun *et al.* (4). The wild type and mutant proteins precipitated with 30–50% saturated ammonium sulfate. The protein pellet was dissolved in TNE buffer and loaded on to a Sephacryl HR-300 gel filtration column (1.8  $\times$  130 cm). The fractions containing  $\alpha$ -crystallin were pooled and subjected to ion exchange chromatography using Mono Q. The purified proteins were dialyzed against the TNE buffer and concentrated by ultrafiltration. The purity of the wild type and deletion mutant proteins was checked by SDS-polyacrylamide gel electrophoresis and found to be homogeneous. The concentrations of the protein samples were determined by the method described by Pace *et al.* (38).

**Chaperone Assays**—The chaperone-like activity of the wild type and mutant proteins was studied using DTT-induced aggregation of insulin. Insulin (0.2 mg/ml) in 10 mM phosphate buffer (pH 7.4) containing 100 mM NaCl in the absence or the presence of chaperones (at the different concentrations mentioned in the figure legends to obtain different chaperone to target protein ratios) was incubated at 37 °C. Aggregation was initiated by adding DTT to a final concentration of 20 mM. The aggregation of the target protein was monitored as right angle light scattering using a Hitachi F-4000 fluorescence spectrophotometer. The samples were placed in the thermostated cuvette holder, and light scattering was measured as a function of time by setting the excitation and emission monochromators at 465 nm with the excitation and emission band passes set at 3 nm.

**Fluorescence Studies**—All fluorescence spectra were recorded using a Hitachi F-4010 fluorescence spectrophotometer with excitation and emission band passes set at 5 and 3 nm, respectively. All spectra were recorded in corrected spectrum mode. Intrinsic tryptophan fluorescence spectra of the wild type and the mutant  $\alpha$ -crystallins (0.15 mg/ml) in 10 mM sodium phosphate buffer (pH 7.4) containing 100 mM NaCl were recorded by exciting the sample with 295-nm light. Urea-induced denaturation of the wild type and deletion mutants of  $\alpha$ -crystallin was studied by monitoring the changes in the tryptophan fluorescence. Proteins at 0.2 mg/ml in 50 mM Tris-HCl buffer (pH 7.2) in the presence of various concentrations of urea were incubated at room temperature (25 °C) for 2 h, and the tryptophan fluorescence spectrum of these samples was recorded with the excitation and emission band passes of 2.5 nm using a Hitachi F-4500 fluorescence spectrophotometer.

To study binding of the hydrophobic probe, bis-ANS, 15  $\mu$ l of 0.8 mM methanolic solution of bis-ANS was added to 1.2 ml of protein sample (as described above), and the samples incubated for 10 min at 37 °C. Fluorescence spectra of the samples were recorded from 400 to 600 nm with the excitation wavelength set at 390 nm.

**Circular Dichroism Studies**—Near- and far-UV CD spectra of the wild type and the mutant  $\alpha$ -crystallins were recorded using a JASCO J-715 spectropolarimeter. Experiments were performed with 1.0 mg/ml protein in TNE buffer using a 1-cm path length cell for the near-UV region and a 0.01-cm path length cell for far-UV region. All spectra reported are the average of five accumulations and are blank corrected.

**Sedimentation through Glycerol Gradient**—Glycerol gradient centrifugation was carried out essentially as described by Lambert *et al.* (39).  $\alpha$ A- or  $\alpha$ B-crystallin and the deletion mutants (1 mg) in TNE buffer (pH 7.4) were loaded on top of a 12-ml linear gradient of glycerol (10–40%) made in the same buffer. The tubes were centrifuged for 18 h at 30,000 rpm in a Beckman SW41 rotor at 4 °C. Fractions (0.3 ml) were withdrawn from the top using a Haake-Buchler Auto Densi-Flow IIC gradient former/remover, and optical density at 280 nm of the fractions was measured using a Shimadzu UV-1601 spectrophotometer. Thyroglobulin (669 kDa), catalase (232 kDa), and aldolase (158 kDa) were used as standards for estimating the molecular masses of the  $\alpha$ -crystallin samples.

**Dynamic Light Scattering Studies**—The hydrodynamic radii of the wild type and the mutant  $\alpha$ -crystallins were measured by dynamic light scattering measurements using a DynaPro MS/X Dynamic Light Scattering Instrument from Protein Solutions Inc. The protein samples were filtered through a 0.22- $\mu$ m filter, and 50  $\mu$ l of 2 mg/ml  $\alpha$ -crystallin sample was used. The cell holder was thermostated at 22 °C. Measurements were made at a fixed angle of 90° using an incident laser beam of 830 nm. Twenty measurements were made with an acquisition time of 10 s for each measurement at the sensitivity of 10%. The data were analyzed using graphical size analysis software, Dynamics, provided with the instrument.

**Subunit Exchange Studies**—The cysteine residues in  $\alpha$ A- and  $\alpha$ Adel-crystallin were covalently labeled with the fluorescence probes, AIAS and LYI, separately by incubating the protein samples (1 mg/ml) in 20 mM MOPS buffer (pH 7.9) containing 100 mM NaCl with a 250  $\mu$ M concentration of the probes at 37 °C for 18 h. The unlabeled probes were removed by passing the samples through a desalting column (PD10), eluted using 50 mM sodium phosphate buffer (pH 7.5) containing 100

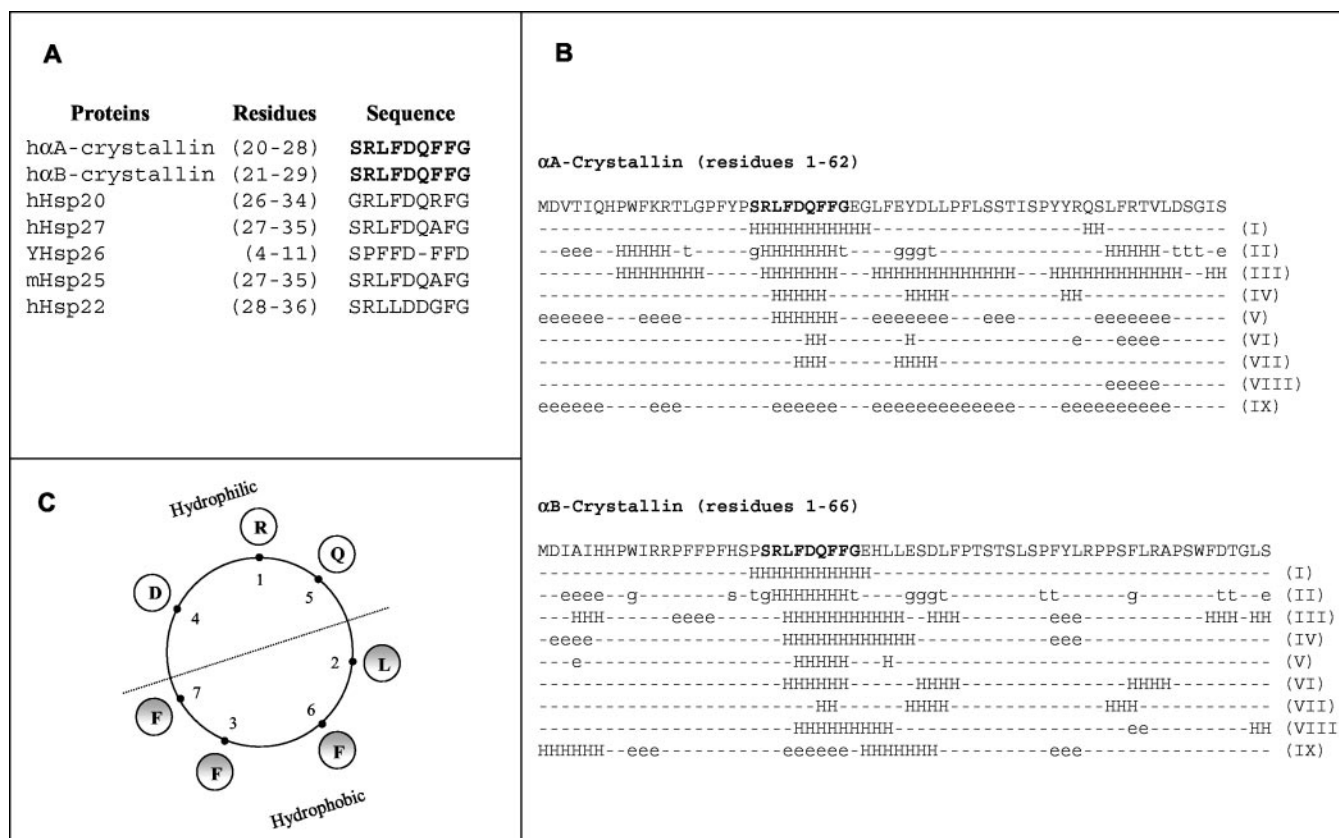


FIG. 1. A, conservation of the RLFQDQFF motif in the N-terminal domains of various small heat shock proteins. B, sequence-based prediction of the secondary structural propensity of the N-terminal domains of  $\alpha$ A- and  $\alpha$ B-crystallin by various programs using different algorithms: UCSC Computational Biology (58) (I), Sspro8 (59) (II), Homology (60–62) (III), hydrophobic moment (using software PepTool Lite 1.1) (IV), nnPredict (63) (V), APSSP2 (64) (VI), PSIPRED (65) (VII), GOR4 (66) (VIII), and Chou-Fasman (67) (IX). The full-length sequences were subjected to prediction methods, and the results of only the N-terminal domains are shown. H, e, t, and g, helix, strand, turn, and  $3_{10}$  helix, respectively. Dashed line, random coil. C, helical wheel representation of the sequence RLFQDQFF showing spatial dispositions of the hydrophobic and hydrophilic residues.

mm NaCl and 1 mM DTT. The void volume fractions containing the labeled protein were pooled, and their concentrations were determined.

Subunit exchange experiments were performed by mixing the AIAS-labeled protein and the LYI-labeled protein at equal concentration (total protein concentration was 0.7 mg/ml) in 50 mM sodium phosphate buffer (pH 7.5) containing 100 mM NaCl and 1 mM DTT and incubating at the indicated temperatures in a Julabo thermostated water bath. 20  $\mu$ l of sample was withdrawn at different time intervals and diluted to 0.4 ml with the same buffer, and the fluorescence spectrum was recorded at room temperature using a Hitachi F4000 fluorescence spectrophotometer with the excitation wavelength of 332 nm in corrected spectrum mode. The excitation and emission band passes were set 5 nm each.

#### RESULTS AND DISCUSSION

Earlier studies indicated that the N-terminal region and the  $\alpha$ -crystallin domains are involved in subunit interactions (40, 41). However, it is not clear which specific sequence(s) in the N-terminal domain is crucial for the quaternary structure of  $\alpha$ -crystallins. In order to identify the peptide regions that might be involved in the subunit interactions, we have earlier screened proteolytic fragments of  $\alpha$ -crystallin for possible interaction with the  $\alpha$ -crystallin heteroaggregate (42). One of the fragments that showed significant interaction is a 27-residue peptide from the N-terminal region. Further analysis showed that this fragment contains RLFQDQFFG, a well conserved motif in the N-terminal region, among the mammalian sHsps (33). Conservation of this motif in many sHsps (Fig. 1A) suggests that it plays a specific role in the structure and function of these proteins. This motif, SRLFDQFFG, is identical in both  $\alpha$ A- and  $\alpha$ B-crystallin. Sequence-based structural prediction with different algorithms shows that this sequence has some propensity to form a helical structure (Fig. 1B). The helical

wheel analysis on the side chain disposition of the residues in the sequence shows that the putative helical segment can exhibit amphipathic character (Fig. 1C). It is important to note that an analogous sequence (residues 7–11) in wheat Hsp16.9, SNVFD, has been found to make contact with residues Trp<sup>48</sup> and Arg<sup>109</sup>-Phe<sup>110</sup> in the “ $\alpha$ -crystallin domain” inter- and intramolecularly (43). It is possible that the corresponding SRLFDQFFG motif in  $\alpha$ A- and  $\alpha$ B-crystallin may have such intra- and intermolecular interactions. Thus, this region in  $\alpha$ A- and  $\alpha$ B-crystallin may be an important determinant of structure and function. In order to investigate the role of this conserved motif, we have created deletion mutants of  $\alpha$ A- and  $\alpha$ B-crystallin, which lack the sequence SRLFDQFFG,  $\alpha$ Adel- or  $\alpha$ Bdel-crystallin, and studied the structure and chaperone-like activity with respect to their wild type counterparts.

We have compared the tryptophan fluorescence spectra of the wild type proteins and deletion mutants of  $\alpha$ A- and  $\alpha$ B-crystallin and found that the spectra of both  $\alpha$ Adel- and  $\alpha$ Bdel-crystallin differ only marginally from those of the respective wild type proteins (data not shown). This result shows that the microenvironment of the tryptophan residues of  $\alpha$ A- and  $\alpha$ B-crystallin does not get altered significantly upon deletion of the sequence SRLFDQFFG. However, this result does not rule out the possibility of tertiary structural alterations in other parts of the molecules. Fig. 2A shows that the near-UV CD spectra of  $\alpha$ A- and  $\alpha$ Adel-crystallin do not overlap with each other and differ in the region between 270 and 300 nm. The difference between near-UV CD spectra of  $\alpha$ B- and  $\alpha$ Bdel-crystallin is more pronounced (Fig. 2B). Drastic changes are observed in the region between 270 and 290 nm.



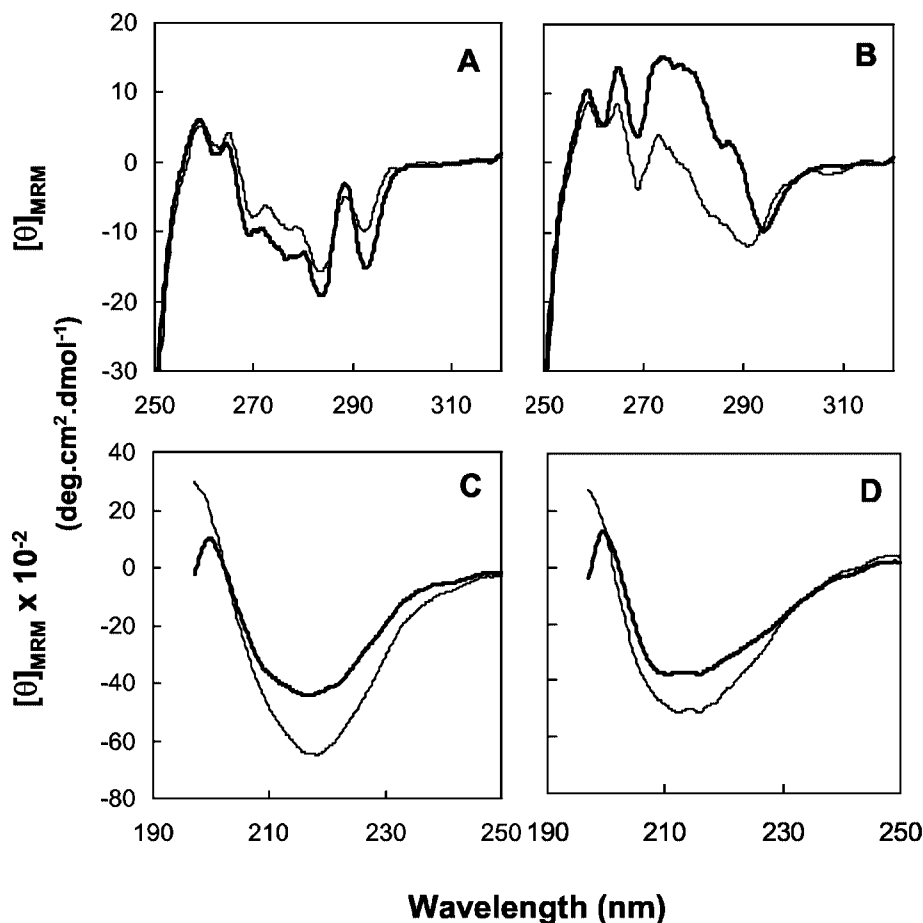


FIG. 2. Near-UV (A and B) and far-UV (C and D) circular dichroism spectra of the wild type proteins and the deletion mutants of  $\alpha$ -crystallins. Spectra were recorded at a protein concentration of 1.0 mg/ml using a 1-cm path length cell for the near-UV region and 0.01-cm path length cell for the far-UV region. A and C,  $\alpha$ A-crystallin (thick solid line) and  $\alpha$ Adel-crystallin (thin solid line). B and D,  $\alpha$ B-crystallin (thick solid line) and  $\alpha$ Bdel-crystallin (thin solid line).  $[\theta]_{\text{MRM}}$ , mean residue mass ellipticity.

The effect of the deletion of the specific conserved sequence, SRLFDQFFG, on the secondary structure of the proteins has been investigated by far-UV CD spectra. In Fig. 2, panels C and D compare the far-UV CD spectra of the mutant and the wild type  $\alpha$ A- and  $\alpha$ B-crystallin, respectively.  $\alpha$ -Crystallins exhibit CD spectra indicative of mainly  $\beta$ -sheet structure with minor content of helical structure (44, 45). As mentioned earlier, sequence-based prediction shows that the deleted specific sequence shows some propensity to form helical structure. It is therefore expected that deletion of this sequence would result in decreased helical content, and since helical structure contributes more toward the observed ellipticity, the far-UV CD spectra of the deletion mutants should exhibit decreased ellipticity. However, the far-UV CD spectra of both  $\alpha$ Adel- and  $\alpha$ Bdel-crystallin show increased ellipticity compared with that of the wild type proteins. This result suggests induction of some secondary structural elements in some regions of the sequence, which could probably arise due to packing alterations upon deletion of the specific sequence.

As mentioned earlier, the N-terminal region and the " $\alpha$ -crystallin domain" are involved in subunit interactions (40, 41). Deletion of the first 56 or 63 residues results in a drastic decrease in the size, whereas truncation of the first 19 residues does not result in significant alteration in the size of  $\alpha$ A-crystallin (36, 37). It therefore appears that the sequence between residues 19 and 56 may contribute significantly to the subunit interactions and hence the oligomeric size of the protein. However, whether some specific sequence(s) within this large segment or the segment as a whole contribute to such intersubunit interactions is not clear. In order to understand the role of the conserved SRLFDQFFG sequence in  $\alpha$ A- and  $\alpha$ B-crystallin in the oligomerization, we have performed glycerol density gradient sedimentation studies and dynamic light

scattering studies on the wild type and the mutant proteins. Fig. 3 compares the sedimentation profiles of the wild type and deletion mutants on a 10–40% glycerol density gradient.  $\alpha$ A-crystallin (Fig. 3A) sediments faster than  $\alpha$ B-crystallin (Fig. 3B), and the molecular masses of these proteins have been estimated to be  $\sim$ 550 and 480-kDa, respectively (see "Experimental Procedures" for details). From the profiles in Fig. 3, A and B, it is evident that the deletion mutants,  $\alpha$ Adel- and  $\alpha$ Bdel-crystallin, sediment much slower compared with the respective wild type proteins, indicating that the deletion mutants exhibit lower molecular mass. It is also to be noted that both  $\alpha$ Adel and  $\alpha$ Bdel show a similar profile and peak at the same position, the estimated molecular mass of these mutants being  $\sim$ 300 kDa.

Table I shows the hydrodynamic radii ( $R_h$ ) and polydispersity of wild type  $\alpha$ A- and  $\alpha$ B-crystallin as well as those of the deletion mutants as measured by dynamic light scattering. The hydrodynamic radius of  $\alpha$ A-crystallin is larger (8.88 nm) than that of  $\alpha$ B-crystallin (7.85 nm). It is seen from Table I that the polydispersity of  $\alpha$ A-crystallin is higher than that of  $\alpha$ B-crystallin. It is evident from Table I that deletion of the conserved SRLFDQFFG sequence results in a decrease in  $R_h$  value as well as the polydispersity in both  $\alpha$ A- and  $\alpha$ B-crystallin.

Thus, our sedimentation and dynamic light scattering studies on the wild type proteins and the deletion mutants clearly show that the conserved SRLFDQFFG sequence in  $\alpha$ A- and  $\alpha$ B-crystallin contributes to the quaternary structure of the protein, especially in higher order subunit assembly. It is important to note that in earlier studies, where 56 or 63 residues were deleted from the N terminus, a drastic decrease in the size leading to dimers and tetramers was observed. Deletion of SRLFDQFFG sequence in  $\alpha$ A- and  $\alpha$ B-crystallin alters the oligomer formation but does not lead to dimers and trimers.

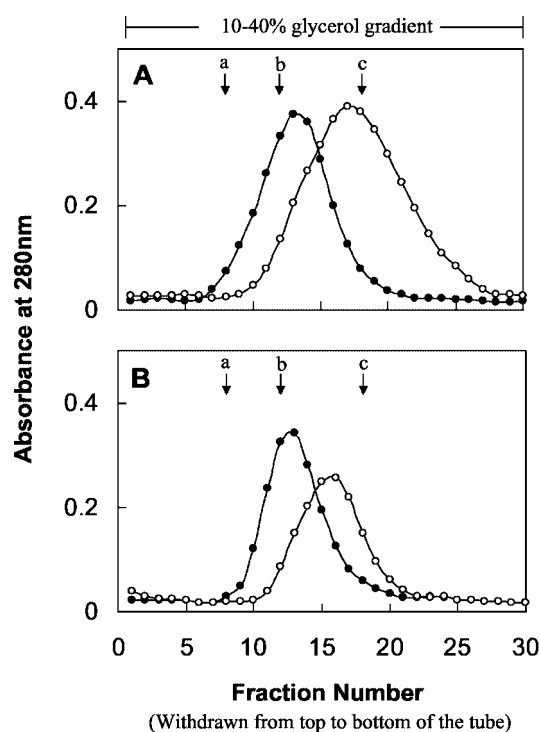


FIG. 3. Sedimentation of the wild type  $\alpha$ -crystallins and the deletion mutants through a linear glycerol gradient (10–40%). A,  $\circ$ ,  $\alpha$ A-crystallin;  $\bullet$ ,  $\alpha$ Adel-crystallin. B,  $\circ$ ,  $\alpha$ B-crystallin;  $\bullet$ ,  $\alpha$ Bdel-crystallin. The positions of proteins used for standard molecular masses are also indicated: aldolase (a) (158 kDa), catalase (b) (232 kDa), and thyroglobulin (c) (669 kDa). See “Experimental Procedures” for details.

TABLE I

Hydrodynamic radius ( $R_h$ ) of the wild type proteins and the deletion mutants of  $\alpha$ A- and  $\alpha$ B-crystallin by dynamic light scattering measurements

The data were analyzed using Dynamics version 5 software.

| Protein                  | $R_h^a$ | Polydispersity <sup>a</sup> | Polydispersity <sup>a</sup> |
|--------------------------|---------|-----------------------------|-----------------------------|
|                          | nm      | nm                          | %                           |
| $\alpha$ A-crystallin    | 8.88    | 2.85                        | 22.17                       |
| $\alpha$ Adel-crystallin | 7.20    | 1.05                        | 14.4                        |
| $\alpha$ B-crystallin    | 7.85    | 1.43                        | 18.2                        |
| $\alpha$ Bdel-crystallin | 7.39    | 1.24                        | 16.6                        |

<sup>a</sup> The values are the averages of three different experimental values. Each experiment value is an average of 20 data accumulations.

Thus, it appears that the rest of the residues in the segment 19–56 contribute other interacting sites in the intersubunit interactions.

In order to find out whether these structural alterations lead to changes in the hydrophobic surfaces on the proteins, we have probed the hydrophobic surfaces using the fluorescent probe, bis-ANS. Upon binding to apolar surfaces, its fluorescence intensity enhances with a blue shift in the emission maximum of its fluorescence spectrum (46). As seen from Fig. 4, the fluorescence intensities of bis-ANS bound to  $\alpha$ Adel- and  $\alpha$ Bdel-crystallin are higher (by  $\sim 20$  and 52%, respectively) than those of bis-ANS bound to  $\alpha$ A- and  $\alpha$ B-crystallin, indicating that the probe binds more to the deletion mutants compared with the wild type proteins. Our result, thus, shows that there are subtle changes in the hydrophobic surfaces upon deletion of the SRLFDQFFG sequence in  $\alpha$ A- and  $\alpha$ B-crystallin.

Thus, significant changes in the secondary, tertiary, and quaternary structure and some changes in surface hydrophobicity of  $\alpha$ A- and  $\alpha$ B-crystallin are observed upon deletion of SRLFDQFFG sequence. We have also investigated the conformational stability of the proteins. Urea-induced denaturation of the wild type and the mutant proteins was monitored by

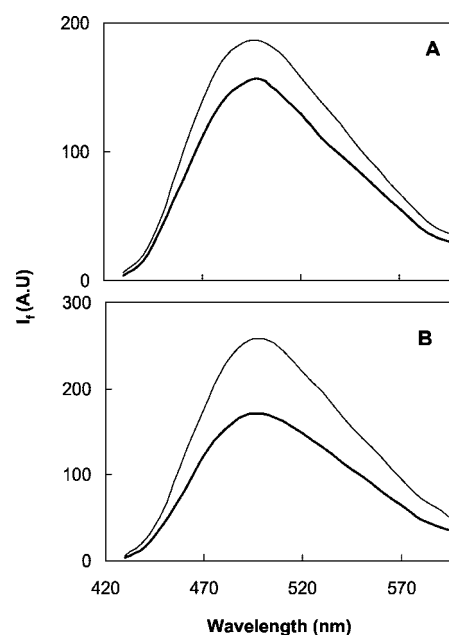


FIG. 4. Fluorescence spectra of bis-ANS bound to  $\alpha$ -crystallins. A, thick line,  $\alpha$ A-crystallin; thin line,  $\alpha$ Adel-crystallin. B, thick line,  $\alpha$ B-crystallin; thin line,  $\alpha$ Bdel-crystallin. The concentrations of  $\alpha$ -crystallins were 0.15 mg/ml. Excitation wavelength was 395 nm.  $I_f$  (A.U.), fluorescence intensity in arbitrary units.

changes in the tryptophan fluorescence. Fig. 5 shows that the deletion mutants are more susceptible to urea-induced denaturation than their respective wild type proteins. This result indicates that the SRLFDQFFG sequence contributes significantly to the overall conformational stability of  $\alpha$ -crystallins.

In order to investigate whether structural and stability alterations lead to changes in function, we have investigated the chaperone-like activity of the wild type and the mutant  $\alpha$ -crystallins toward DTT-induced aggregation of insulin at 37 °C (Fig. 6A). It is seen from the figure that the chaperone-like activity of  $\alpha$ B-crystallin is higher than that of  $\alpha$ A-crystallin, consistent with the earlier reports on the chaperone-like activity of these proteins (4, 14, 17, 18); a 1:1 weight ratio of  $\alpha$ A-crystallin to insulin is required to obtain about 80% protection, whereas only a 0.4:1 ratio of  $\alpha$ B-crystallin to insulin is required to obtain similar protection. Interestingly, both the mutants,  $\alpha$ Adel- and  $\alpha$ Bdel-crystallin, exhibit enhanced chaperone-like activity compared with that of the wild type proteins.  $\alpha$ Bdel-crystallin, however, is more active compared with  $\alpha$ Adel-crystallin (Fig. 6A). The concentrations or the weight ratios of the chaperones to target protein required to get a comparable extent of protection differ quite significantly and also vary with temperature. Therefore, deriving a parameter using the chaperone activity data at different ratios under a given set of experimental conditions would be useful in order to make a meaningful comparison. The ratio of target protein concentration to the chaperone concentration would reflect the efficiency of the chaperone. We have therefore compared the weight ratio of the target protein to the chaperone at 50% protection of the aggregation. Fig. 6B compares the chaperone efficiencies of the wild type and the deletion mutant proteins. From the figure it is evident that the chaperone efficiency of  $\alpha$ A- and  $\alpha$ B-crystallin are increased severalfold upon deletion of the SRLFDQFFG sequence; the chaperone efficiency of  $\alpha$ Adel-crystallin is 8.4-fold higher than that of  $\alpha$ A-crystallin, and that of  $\alpha$ Bdel-crystallin is 6.0-fold higher than that of  $\alpha$ B-crystallin. Thus, the  $\sim$ fold increase in the chaperone-like activity of  $\alpha$ A-crystallin upon deletion of the SRLFDQFFG sequence is higher than that observed for  $\alpha$ B-crystallin.

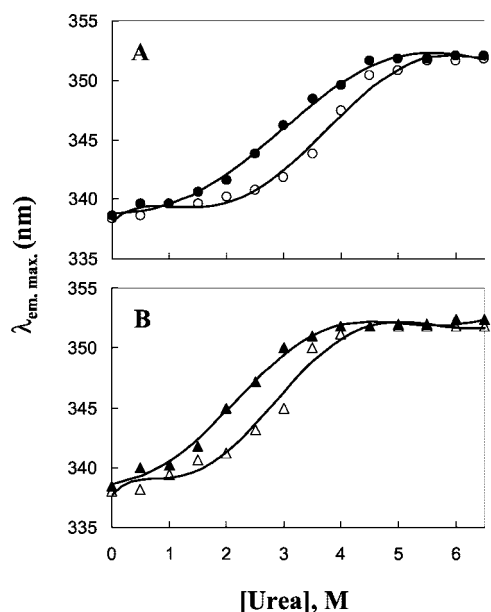


FIG. 5. Urea-induced denaturation of the wild type and the deletion mutant of  $\alpha$ A-crystallins (A) and  $\alpha$ B-crystallins (B) monitored by intrinsic tryptophan fluorescence.  $\circ$ ,  $\alpha$ A-crystallin;  $\bullet$ ,  $\alpha$ Adel-crystallin;  $\triangle$ ,  $\alpha$ B-crystallin;  $\blacktriangle$ ,  $\alpha$ Bdel-crystallin.  $\lambda_{em. max.}$ , wavelength of emission maximum.

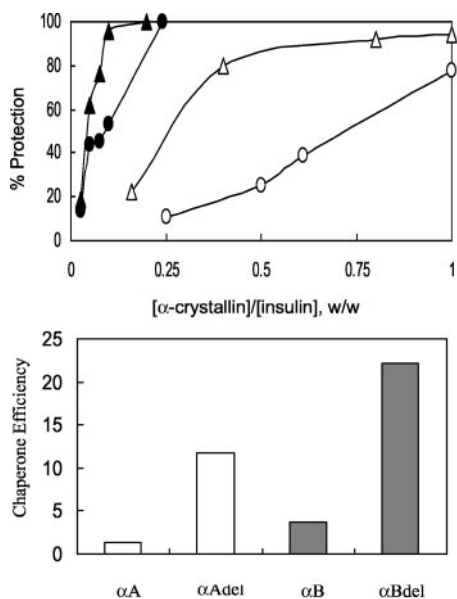


FIG. 6. Chaperone-like activity of wild type  $\alpha$ A- and  $\alpha$ B-crystallins and the deletion mutants toward DTT-induced aggregation of insulin. A,  $\circ$ ,  $\alpha$ A-crystallin;  $\bullet$ ,  $\alpha$ Adel-crystallin;  $\triangle$ ,  $\alpha$ B-crystallin;  $\blacktriangle$ ,  $\alpha$ Bdel-crystallin. % Protection, the percentage prevention of aggregation of insulin by  $\alpha$ -crystallins as measured by light scattering. B, comparison of "chaperone efficiency," the weight ratio of target protein to chaperone for 50% prevention of aggregation.

As mentioned earlier,  $\alpha$ -crystallins exhibit temperature-dependent chaperone-like activity (13, 19, 22). At 25 °C, both  $\alpha$ A- and  $\alpha$ B-crystallin exhibit less chaperone-like activity; at a 1:1 weight ratio of  $\alpha$ -crystallins to insulin, the percentage of protection was found to be 9.2 and 16.3% in the case of  $\alpha$ A- and  $\alpha$ B-crystallin, respectively. However, even at a 0.5:1 weight ratio, the percentage of protection observed in the cases of  $\alpha$ Adel- and  $\alpha$ Bdel-crystallin was 47.5 and 95.7, respectively. Thus, these results show that the deletion mutants exhibit enhanced activity even at the lower temperature (25 °C).

One of the characteristic features that small heat shock

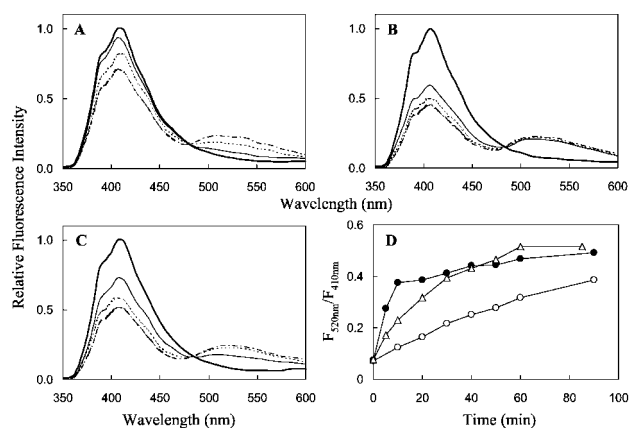
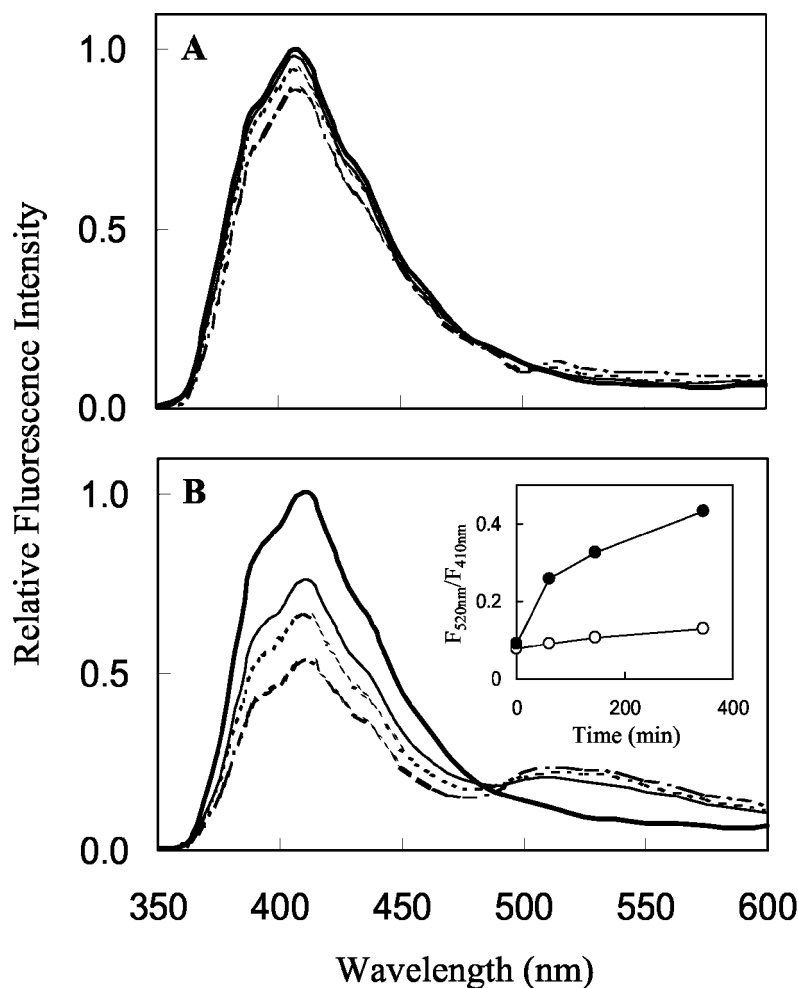


FIG. 7. Subunit exchange in  $\alpha$ A- and  $\alpha$ Adel-crystallin at 37 °C monitored by FRET. A mixture (0.35 mg/ml each) of AIAS-labeled protein (donor) and LYI-labeled protein (acceptor) was incubated at 37 °C; a 20- $\mu$ l sample was withdrawn at the indicated time intervals and diluted to 0.4 ml with phosphate buffer, and the fluorescence spectrum was recorded at room temperature (25 °C) with the excitation wavelength of 332 nm. Subunit exchange in  $\alpha$ A-crystallin (A),  $\alpha$ Adel-crystallin (B), and between  $\alpha$ A- and  $\alpha$ Adel-crystallins (C). Thick solid line, spectrum recorded immediately after mixing; thin solid line, 10-min incubation; dotted line, 30-min incubation; dotted and dashed line, 60-min incubation. D, comparison of subunit exchange in  $\alpha$ A- ( $\circ$ ) and  $\alpha$ Adel-crystallins ( $\bullet$ ) and in between  $\alpha$ A- and  $\alpha$ Adel-crystallins ( $\triangle$ ) as a function of time.  $F_{520nm}/F_{410nm}$  represents the ratio of fluorescence intensities at 520 to 410 nm of the fluorescence spectrum.

proteins exhibit is that subunits of one sHsp can exchange between the multimers of the same protein or with subunits of other related sHsps. Although the exact role of this dynamic property is not clear, it appears to be of some functional importance, since  $\alpha$ B-crystallin and Hsp25/27 form heteromultimers with one another *in vivo* (47–50). We therefore studied the dynamic property of subunit exchange of the wild type and the deletion mutants. Bova *et al.* (48) have shown that the subunit exchange of rat  $\alpha$ A-crystallin can be monitored using FRET by labeling the single cysteine residue by AIAS as donor and LYI as acceptor fluorescent probes. The human  $\alpha$ A-crystallin has two cysteine residues at positions 131 and 142, whereas  $\alpha$ B-crystallin does not have any cysteine residues in its sequence. We have therefore studied the subunit exchange only in the wild type and the mutant  $\alpha$ A-crystallin. We have labeled one batch of the proteins with AIAS and the other with LYI and mixed these two labeled  $\alpha$ A-crystallin or mutant in a 1:1 weight ratio at the indicated temperature and monitored the subunit exchange by FRET at 37 °C. As shown in Fig. 7, while the exchange progresses, the fluorescence intensity of donor decreases with a concomitant increase in the acceptor fluorescence upon exciting the sample with the donor absorption maximum, 332 nm. The ratio of the fluorescence intensity at the emission maximum of the acceptor LYI (520 nm) to that of the donor AIAS (410 nm) monitored as a function of incubation time would thus reflect on the rate of subunit exchange. It is seen from Fig. 7 (A, B, and D) that the rate of subunit exchange between the homomultimers of  $\alpha$ Adel-crystallin is significantly higher than that between homomultimers of  $\alpha$ A-crystallin. Thus, it is evident from our results that the SRLFDQFFG sequence not only determines the higher order assembly but also contributes to a significant extent to the stability or the architecture of the oligomeric assembly, since the deletion of this region results in increased dynamic nature of the assembly. We have also investigated whether the wild type and the mutant  $\alpha$ A-crystallin can exchange their subunits with each other. Fig. 7 (C and D) shows clearly that both  $\alpha$ A- and  $\alpha$ Adel-crystallin exchange their subunits to form a heteroassembly. From the initial slope of the curves in Fig. 7D, it appears that

FIG. 8. Subunit exchange in  $\alpha$ A-crystallin (A) and  $\alpha$ Adel-crystallin (B) at 25 °C monitored by FRET. A mixture (0.35 mg/ml each) of AIAS-labeled protein (donor) and LYI-labeled protein (acceptor) was incubated at 25 °C; a 20- $\mu$ l sample was withdrawn at the indicated time intervals and diluted to 0.4 ml with phosphate buffer, and the fluorescence spectrum was recorded at room temperature (25 °C) with an excitation wavelength of 332 nm. *Thick solid line*, spectrum recorded immediately after mixing; *thin solid line*, 60-min incubation; *dotted line*, 145-min incubation; *dashed and dashed line*, 345-min incubation. *Inset in B*, variation of the ratio of fluorescence intensities at 520 to 410 nm ( $F_{520\text{ nm}}/F_{410\text{ nm}}$ ) of the fluorescence spectra as a function of time. *Open circle*,  $\alpha$ A-crystallin; *closed circle*,  $\alpha$ Adel-crystallin.



the rate of exchange of subunits between the wild type and mutant protein lies between that of the individual homomultimers of  $\alpha$ A- or  $\alpha$ Adel-crystallin.

We have also investigated the subunit exchange at 25 °C. As seen from Fig. 8, subunit exchange in  $\alpha$ A-crystallin is not significant at 25 °C, whereas it is quite significant in the case of  $\alpha$ Adel-crystallin, although it is slower compared with that at 37 °C. It is evident from earlier studies that temperature-induced increase in the rate of subunit exchange in  $\alpha$ -crystallin (47, 48, 50) parallels the temperature-induced increase in the chaperone-like activity (13). The dynamic properties of subunit assembly in sHsps are important for their activity (51, 52). Our results of enhanced chaperone-like activity of deletion mutant of  $\alpha$ A-crystallin correlate well with the increased rate of subunit exchange of the multimeric assembly.

Masking and unmasking the chaperone sites under certain conditions might be a mode of regulation of the activities of heat shock proteins. Destabilization of the multimeric assembly by temperature and other post-translational modifications such as phosphorylation appears to alter the structure and the activity of several molecular chaperones and heat shock proteins (43, 53–57). It is therefore important to understand the local structures or sequences that are critical in determining the structure and function of the molecule. Our study shows that the SRLFDQFFG sequence may be at least one such critical motif present in small heat shock proteins, particularly in  $\alpha$ A- and  $\alpha$ B-crystallin, and changes around this region such as phosphorylation may be regulatory in nature. It is important to note that one of the phosphorylatable serines is the residue before the SRLFDQFFG sequence in  $\alpha$ B-crystallin. It is possi-

ble that phosphorylation of this residue may change the interaction of the sequence with other parts of the molecule and hence modulate the structure and the chaperone-like activity of the protein.

We conclude that the putative amphipathic helical sequence, SRLFDQFFG, at the N-terminal domain of  $\alpha$ -crystallins contributes to the higher order assembly of their subunits as well as structural stability. Interestingly, the mutants exhibit increased chaperone-like activity, increased exposed hydrophobic surfaces, and increased rate of subunit exchange compared with the wild type proteins. It appears that loosening of subunit organization leading to more dynamic properties enhances the available chaperone sites for the target proteins.

*Acknowledgments*—We thank Dr. G. Krishnamoorthy and Rama Reddy (Tata Institute of Fundamental Research, Mumbai, India) for help in dynamic light scattering studies. We also thank Dr. V. Srinivas for help in the initial labeling experiments.

#### REFERENCES

- Quax-Jeuken, Y., Quax, W., van Rens, G., Khan, P. M., and Bloemendal, H. (1985) *Proc. Natl. Acad. Sci. U. S. A.* **82**, 5819–5823
- Bloemendal, H. (1981) in *Molecular and Cellular Biology of the Eye Lens* (Bloemendal, H., ed) pp. 1–41, John Wiley and Sons, Inc., New York
- Bhat, S. P., Horwitz, J., Srinivasan, A., and Ding, L. (1991) *Eur. J. Biochem.* **202**, 775–781
- Sun, T. X., Das, B. K., and Liang, J. J. (1997) *J. Biol. Chem.* **272**, 6220–6225
- Bhat, S. P., and Nagineni, C. N. (1989) *Biochem. Biophys. Res. Commun.* **158**, 319–325
- Kato, K., Shinohara, H., Kurobe, N., Goto, S., Inaguma, Y., and Ohshima, K. (1991) *Biochim. Biophys. Acta* **1080**, 173–180
- Ingolia, T. D., Craig, E. A. (1982) *Proc. Natl. Acad. Sci. U. S. A.* **79**, 2360–2364
- Klemenz, R., Frohli, E., Steiger, R. H., Schafer, R., and Aoyama, A. (1991) *Proc. Natl. Acad. Sci. U. S. A.* **88**, 3652–3656
- Horwitz J. (1992) *Proc. Natl. Acad. Sci. U. S. A.* **89**, 10449–10453



10. Dasgupta, S., Hohman, T. C., and Carper, D. (1992) *Exp. Eye Res.* **54**, 461–470
11. Martin, J. L., Mestrlil, R., Hilal-Dandan, R., Brunton, L. L., and Dillmann, W. H. (1997) *Circulation* **96**, 4343–4348
12. Clark, J. I., and Muchowski, P. J. (2000) *Curr. Opin. Struct. Biol.* **10**, 52–59
13. Raman, B., and Rao, C. M. (1994) *J. Biol. Chem.* **269**, 27264–27268
14. Datta, S. A., and Rao, C. M. (1999) *J. Biol. Chem.* **274**, 34773–34778
15. Rajaraman, K., Raman, B., and Rao, C. M. (1996) *J. Biol. Chem.* **271**, 27595–27600
16. Das, K. P., Petrash, J. M., and Surewicz, W. K. (1996) *J. Biol. Chem.* **271**, 10449–10452
17. Rajaraman, K., Raman, B., Ramakrishna, T., and Rao, C. M. (1998) *Biochem. Biophys. Res. Commun.* **249**, 917–921
18. Goenka, S., Raman, B., Ramakrishna, T., and Rao, C. M. (2001) *Biochem. J.* **359**, 547–556
19. Raman, B., Ramakrishna, T., and Rao, C. M. (1995) *FEBS Lett.* **365**, 133–136
20. Raman, B., and Rao, C. M. (1997) *J. Biol. Chem.* **272**, 23559–23564
21. Smith, J. B., Liu, Y., and Smith, D. L. (1996) *Exp. Eye Res.* **63**, 125–128
22. Das, K. P., and Surewicz, W. K. (1995) *FEBS Lett.* **369**, 321–325
23. Rajaraman, K., Raman, B., Ramakrishna, T., and Rao, C. M. (2001) *FEBS Lett.* **497**, 118–123
24. Hook, D. W. A., and Harding, J. J. (1997) *Eur. J. Biochem.* **247**, 380–385
25. Hess, J. F., and Fitzgerald, P. G. (1998) *Mol. Vis.* **4**, 29–32
26. Marini, I., Moschini, R., Del Corso, A., and Mura, U. (2000) *J. Biol. Chem.* **275**, 32559–32565
27. Narberhaus, F. (2002) *Microbiol. Mol. Biol. Rev.* **66**, 64–93
28. Kumar, L. V., Ramakrishna, T., and Rao, C. M. (1999) *J. Biol. Chem.* **274**, 24137–24141
29. Bova, M. P., Yaron, O., Huang, Q., Ding, L., Haley, D. A., Stewart, P. L., and Horwitz, J. (1999) *Proc. Natl. Acad. Sci. U. S. A.* **96**, 6137–6142
30. Vicart, P., Caron, A., Guicheney, P., Li, Z., Prevost, M. C., Faure, A., Chateau, D., Chapon, F., Tome, F., Dupret, J. M., Paulin, D., and Fardeau, M. (1998) *Nat. Genet.* **20**, 92–95
31. Litt, M., Kramer, P., LaMorticella, D. M., Murphey, W., Lovrien, E. W., and Weleber, R. G. (1998) *Hum. Mol. Genet.* **7**, 471–474
32. Andley, U. P., Patel, H. C., and Xi, J. H. (2002) *J. Biol. Chem.* **277**, 10178–10186
33. de Jong, W. W., Caspers, G. J., and Leunissen, J. A. (1998) *Int. J. Biol. Macromol.* **22**, 151–162
34. Smulders, R. H. P. H., Carver, J. A., Lindner, R. A., van Boekel, M. A., Bloemendal, H., and de Jong, W. W. (1996) *J. Biol. Chem.* **271**, 29060–29066
35. Pasta, S. Y., Raman, B., Ramakrishna, T., and Rao, C. M. (2002) *J. Biol. Chem.* **277**, 45821–45828
36. Merck, K. B., De Haard-Hoekman, W. A., Oude Essink, B. B., Bloemendal, H., and de Jong, W. W. (1992) *Biochim. Biophys. Acta* **1130**, 267–276
37. Bova, M. P., Mchaourab, H. S., Han, Y., and Fung, B. K. (2000) *J. Biol. Chem.* **275**, 1035–1042
38. Pace, N. C., Vajdos, F., Fee, L., Grimsley, G., and Gray, T. (1995) *Protein Sci.* **4**, 2411–2423
39. Lambert, H., Charette, S. J., Bernier, A. F., Guimond, A., and Landry, J. (1999) *J. Biol. Chem.* **274**, 9378–9385
40. Feil, I. K., Malfois, M., Hendle, J., van Der Zandt, H., and Svergun, D. I. (2001) *J. Biol. Chem.* **276**, 12024–12029
41. Berengian, A. R., Bova, M. P., and Mchaourab, H. S. (1997) *Biochemistry* **36**, 9951–9957
42. Datta, S. A., (2000) *Molecular Chaperone-like Activity of Homo- and Hetero-oligomers of  $\alpha$ A- and  $\alpha$ B-crystallins*. Ph.D. thesis, Jawaharlal Nehru University, New Delhi, India
43. van Montfort, R. L., Basha, E., Friedrich, K. L., Slingsby, C., and Vierling, E. (2001) *Nat. Struct. Biol.* **8**, 1025–1030
44. Liang, J. N., and Chakrabarti, B. (1982) *Biochemistry* **21**, 1847–1852
45. Li, L. K., and Spector, A. (1974) *Exp. Eye Res.* **19**, 49–57
46. Musci, G., Metz, G. D., Tsunematsu, H., and Berliner, L. J. (1985) *Biochemistry* **24**, 2034–2039
47. van den Oetelaar, P. J., van Someren, P. F., Thomson, J. A., Siezen, R. J., and Hoenders, H. J. (1990) *Biochemistry* **29**, 3488–3493
48. Bova, M. P., Ding, L. L., Horwitz, J., and Fung, B. K. (1997) *J. Biol. Chem.* **272**, 29511–29517
49. Sun, T. X., and Liang, J. J. (1998) *J. Biol. Chem.* **273**, 286–290
50. Sun, T. X., Akhtar, N. J., and Liang, J. J. (1998) *FEBS Lett.* **430**, 401–404
51. Bova, M. P., Huang, Q., Ding, L., and Horwitz, J. (2002) *J. Biol. Chem.* **277**, 38468–38475
52. Gu, L., Abulimiti, A., Li, W., and Chang, Z. (2002) *J. Mol. Biol.* **319**, 517–526
53. Ito, H., Kamei, K., Iwamoto, I., Inaguma, Y., Nohara, D., and Kato, K. (2001) *J. Biol. Chem.* **276**, 5346–5352
54. Leung, S. M., Senisterra, G., Ritchie, K. P., Sadis, S. E., Lepock, J. R., and Hightower, L. E. (1996) *Cell Stress Chaperones* **1**, 78–89
55. Yonehara, M., Minami, Y., Kawata, Y., Nagai, J., and Yahara, I. (1996) *J. Biol. Chem.* **271**, 2641–2645
56. Brunschier, R., Danner, M., and Seckler, R. (1993) *J. Biol. Chem.* **268**, 2767–2772
57. Hansen, J. E., and Gafni, A. (1994) *J. Biol. Chem.* **269**, 6286–6289
58. Fischer, D., Barret, C., Bryson, K., Elofsson, A., Godzik, A., Jones, D., Karplus, K. J., Kelley, L. A., MacCallum, R. M., Pawowski, K., Rost, B., Rychlewski, L., and Sternberg, M. (1999) *Proteins Suppl.* **3**, 209–217
59. Baldi, P., Brunak, S., Frasconi, P., Pollastri, G., and Soda, G. (1999) *Bioinformatics* **15**, 937–946
60. Nishikawa, K., and Ooi, T. (1986) *Biochim. Biophys. Acta* **871**, 45–54
61. Sweet, R. M. (1986) *Biopolymers* **25**, 1565–1577
62. Levin, J. M., Robson, B., and Garnier, J. (1986) *FEBS Lett.* **205**, 303–308
63. Kneller, D. G., Cohen, F. E., and Langridge, R. (1990) *J. Mol. Biol.* **214**, 171–182
64. Raghava, G. P., Solanki, R. J., Soni, V., and Agrawal, P. (2000) *BioTechniques* **29**, 108–116
65. McGuffin, L. J., Bryson, K., and Jones, D. T. (2000) *Bioinformatics* **16**, 404–405
66. Garnier, J., Gibrat, J.-F., and Robson, B. (1996) *Methods Enzymol.* **266**, 540–553
67. Chou, P. Y., and Fasman, G. D. (1978) *Annu. Rev. Biochem.* **47**, 251–276